J Geod
DOI 10.1007/s00190-008-0250-9

ORIGINAL ARTICLE

Error-covariances of the estimates of spherical harmonic coefficients computed by LSC, using second-order radial derivative functionals associated with realistic GOCE orbits

D. N. Arabelos · C. C. Tscherning

Received: 16 August 2007 / Accepted: 14 July 2008

Abstract Least-squares collocation may be used for the estimation of spherical harmonic coefficients and their error and error correlations from GOCE data. Due to the extremely large number of data, this requires the use of the so-called method of Fast Spherical Collocation (FSC) which requires that data is gridded equidistantly on each parallel and have the same uncorrelated noise on the parallel. A consequence of this is that error-covariances will be zero except between coefficients of the same signed order (i.e., the same order and the same coefficient type C–C or S–S). If the data distribution and the characteristics of the data noise are symmetric with respect to the equator, then, within a given order and coefficient type, the error-covariances amongst coefficients whose degrees are of different parity also vanish. The deviation from this "ideal" pattern has been studied using data-sets of second order radial derivatives of the anomalous potential. A total number of points below 17,000 were used having an equi-angular or an equal area distribution or being associated with points on a realistic GOCE orbit but close to the nodes of a grid. Also the data were considered having a correlated or an uncorrelated noise and three different signal covariance functions. Grids including data or not including data in the polar areas were used. Using the functionals associated with the data, error estimates of coefficients and error-correlations between coefficients were calculated up to a maximal degree and order equal to 90. As expected, for the data-distributions with no data in the polar areas the error-estimates were found to be larger than when the polar areas contained data. In all cases it was found that only the error-correlations between coefficients of the same order were significantly different from zero (up to 88%). Error-correlations were significantly larger when data had been regarded as having non-zero error-correlations. Also the error-correlations were largest when the covariance function with the largest signal covariance distance was used. The main finding of this study was that the correlated noise has more pronounced impact on gridded data than on data distributed on a realistic GOCE orbit. This is useful information for methods using gridded data, such as FSC.

Keywords Spherical harmonic coefficients · Least-Squares Collocation · GOCE gradiometer data · Error-covariances

D. N. Arabelos (✉)
Department of Geodesy and Surveying,
Aristotle University of Thessaloniki,
54124 Thessaloniki, Greece
e-mail: arab@eng.auth.gr

C. C. Tscherning
Niels Bohr Institute, University of Copenhagen,
Juliane Maries vej 32, 2100 Copenhagen Oe, Denmark
e-mail: cct@gfy.ku.dk

1 Introduction

The method of Least-Squares Collocation, LSC, Moritz (1980) and Tscherning (2001) may be used for the estimation of the spherical harmonic coefficients C_{ij} of the anomalous gravity potential,

$$T(\overline{\varphi}, \lambda, r) = \frac{GM}{r} \sum_{i=2}^{\infty} \left(\frac{a}{r}\right)^i \sum_{j=-i}^{i} \overline{P}_{ij}(\sin \overline{\varphi})[C_{ij} e_j(\lambda)], \quad (1)$$

where $\overline{\varphi}$ is the geocentric latitude, λ the longitude, r the radial distance, a the semi-major axis (or similar scaling constant), $\overline{P}_{ij}$ the fully normalized associated Legendre function of degree i and order j, GM the product of the gravitational constant and the mass of the Earth and

$$e_j(\lambda) = \begin{cases} \cos(j\lambda) & \text{for } j \geq 0, \\ \sin(|j|\lambda) & \text{for } j < 0. \end{cases}$$

LSC requires the knowledge of an estimate of the covariance function of the anomalous gravity potential,

$$\operatorname{cov}(T(P), T(Q)) = \sum_{i=2}^{\infty} \left(\frac{R^2}{rr'}\right)^{i+1} \sigma_i^2 P_i(\cos\psi), \tag{2}$$

where P, Q are points in space with geocentric radial distances r and r' respectively, and separated by spherical distance ψ, R is the radius of a sphere inside the Earth, σ_i^2 are the so-called degree variances

$$\sigma_i^2 = \sum_{j=-i}^{i} C_{ij}^2 \left(\frac{a}{R}\right)^{2i+2} \tag{3}$$

and P_i are the Legendre polynomials. From (2), covariances of other quantities are obtained by covariance-propagation, i.e., the associated linear functionals are applied to the basic covariance function. For covariances between a coefficient and an observation such as point values of T, the radial derivative, the second-order radial derivative or the derivatives with respect to latitude, the covariance becomes Tscherning (2001)

$$\begin{aligned} \operatorname{cov}(C_{ij}, \text{obs}_m) &= \frac{c_m^i}{r} \left(\frac{a}{r}\right)^i \overline{P}_{ij}^n(\sin\overline{\varphi}) e_j(\lambda) \\ &= u(r, \overline{\varphi}) e_j(\lambda), \end{aligned} \tag{4}$$

where c_m^i depends on the type of observation m and on the degree i, $\overline{P}_{ij}^n$ is the nth derivative of the Legendre function with respect to the latitude. In the case of the second radial derivatives which are used in the paper, it holds that

$$c_m^i = \frac{GM}{r^2}(i+1)(i+2)\sigma_i^2.$$

The estimated coefficient is obtained using

$$\begin{aligned} \widetilde{C}_{ij} &= \{\operatorname{cov}(C_{ij}, \text{obs}_m)\}^T \{\operatorname{cov}(\text{obs}_k, \text{obs}_m) + \tau_{km}\}^{-1} \{g_m\} \\ &= \{b_m^{ij}\}^T \{g_m\}, \end{aligned} \tag{5}$$

where g_k are the observations and τ_{km} are the data noise covariances.

The use of LSC requires, as seen from (5), that a linear system of equations with as many unknowns as the number of observations is solved. This is a drawback of this method, related to the current ability of the computers in handling the very large (full) systems of linear equations produced when large amount of data are used.

On the other hand, LSC is a flexible method for the computation not only of the harmonic coefficients but also of their error and error-covariance estimates from any kind of data related to the gravity field, without any formal requirement about their distribution. Furthermore, LSC estimates have minimum square errors and it is the only method for which it has been proved that the method converges (Sansò and Tscherning 1980). This is very important when data from satellite missions are to be used, such as Satellite Gravity Gradiometer (SGG) data from GOCE (Johannesen et al. 2003).

The large amount of data has made the use of the method of FSC (Sansò and Tscherning 2003) necessary. However this LSC method requires data to be gridded equidistantly in longitude and the noise has to be uncorrelated and uniform on each parallel. Therefore, an aim of this paper is to investigate the consequences of these assumptions on the derived error estimates. We will do this by comparing with results obtained using "full-fledged" LSC, however solving systems with a relatively small number of equations.

In an earlier paper (Arabelos and Tscherning 2007), a strategy was discussed for the selection of point data on a realistic GOCE orbit, leading to optimal LSC determination of spherical harmonic coefficients with the minimum number of data points. In the framework of this investigation, numerical experiments were carried out using simulated SGG data with uncorrelated or correlated noise. Spherical harmonic expansions were determined, using different data distributions. The suggested strategy was based on the comparison between computed and true coefficients, the collocation standard deviation of the estimation error of the coefficients and the comparison of the original data with data generated by the computed coefficients. One of the conclusions of this investigation was that the quality of the harmonic coefficients predicted from data on equal- (or nearly equal) area grids is similar or even better than the quality of coefficients predicted from data on equiangular grids, although in the last case a considerably larger amount of data is used.

Here we only study error estimates and error correlations as a function of the different distributions and whether correlation has been assumed or not. Hence, only the signal covariance function (2) and the error covariance function play a role, not the observation itself.

In the present paper error-covariances of the estimates of all spherical harmonic coefficients determined in Arabelos and Tscherning (2007) are computed which may aid in understanding the impact of the data distribution and noise characteristics on the harmonic coefficients predicted by LSC. Section 2 describes the general formulas for the computation of error covariances and the special case for equiangular gridded data. Section 3 shows the results of the computations in terms of error-estimates of coefficients and of error-correlations of coefficients of a certain degree and order with other coefficients. Note that we are not here considering whether it is feasible or not to use full-fledged LSC to estimate a gravity field from GOCE data. Finally, conclusions based on the results of Sect. 3 are given in Sect. 4.

2 Calculation of error-covariances

For $(i \neq r) \vee (j \neq t)$ the error-covariances (Heiskanen and Moritz 1967) (e.g., eq. 7-65) are equal to

$$\mathrm{ecov}(ij, rt) = -\{b_m^{ij}\}^T \{\mathrm{cov}(C_{rt}, g_m)\}, \tag{6}$$

where we have assumed the original coefficients to be uncorrelated. One has to add the respective degree variance in order to obtain the error variance of a predicted quantity.

For data gridded equidistantly in longitude and uniform and uncorrelated noise on and between each parallel or if the noise depends only on the longitude distance between observation points, the covariances are equal to a product of three quantities, a constant $u(r_k, \overline{\varphi}_k)$ for each parallel k, s_k the solution vector of the subsystem corresponding to each order j and $e_t(l\Delta\lambda)$, see (4), such that

$$\mathrm{ecov}(ij, rt) = -\sum_k u_k(r, \overline{\varphi}) s_k \sum_l e_j(l\Delta\lambda) e_t(l\Delta\lambda). \tag{7}$$

The last sum in (7) is zero except for $j = t$. It is equal to M for $i = 0$ and otherwise equal to $M/2$, where M is the number of the parallels (Sansò and Tscherning 2003) (Eqs. B9 and B10). This was already proved (under less general assumptions) in Colombo (1981).

If the parallels are ordered symmetrically around equator, the error-covariances for odd or even degree i and vice-versa may be close to zero because the associated Legendre functions, or their derivatives in this case, have opposite sign in each hemisphere. If the error estimates associated with the data also are symmetric with respect to the equator, the error-covariances become identical to zero. In this case, we may write (6) as (with subscript n for the Northern Hemisphere and s for the Southern Hemisphere)

$$\mathrm{ecov}(ij, rt) = -\begin{pmatrix} C_{n,ij} \\ C_{s,ij} \end{pmatrix}^T \begin{pmatrix} C_{nn} & C_{ns} \\ C_{ns} & C_{ss} \end{pmatrix}^{-1} \begin{pmatrix} C_{n,rt} \\ C_{s,rt} \end{pmatrix}, \tag{8}$$

where $C_{nn} = C_{ss}, C_{n,ij} = p\, C_{s,ij}, C_{n,rt} = kC_{s,rt}$, with $p = 1$ for even i and -1 for odd i, $k = 1$ for even r and -1 for odd r if the observations are not derivatives with respect to latitude. Evaluation of (8) in this case will show that the error-covariance is zero when i and k have opposite signs. If the observations are associated with derivatives with respect to latitude, a similar combination of even and odd orders i and k will also result in zero error-covariances.

From the error covariances $\mathrm{ecov}(ij, rt)$ the error-correlations $\mathrm{ecorr}(ij, rt)$ are computed for $(i \neq r) \vee (j \neq t)$ according to the formula

$$\mathrm{ecorr}(ij, rt) = \frac{\mathrm{ecov}(ij, rt)}{\sigma(C_{ij})\sigma(C_{rt})}, \tag{9}$$

where $\mathrm{ecorr}(ij, rt)$ is the error-correlation between the spherical harmonic coefficients C_{ij} and C_{rt}, $\mathrm{ecov}(ij, rt)$ stands for the corresponding error-covariance and $\sigma(C_{ij})$ and $\sigma(C_{rt})$ are the error estimates of the spherical harmonic coefficients C_{ij} and C_{rt} respectively.

3 Numerical results

In the following, numerical experiments using T_{rr} data sets are described. A detailed description of these data sets is given in Arabelos and Tscherning (2007). Here, only information about the distribution, the amount of the data points and the noise characteristics of the data set related to corresponding numerical experiment are summarized. The decimation of the data on a realistic GOCE orbit was carried out selecting for each node of the corresponding grid the data point lying closest (up to a predefined distance) to this node (see Table 1). In this way the data points were retained in their original positions and the distribution was more or less homogeneous.

The low degree harmonics up to degree 24, 50 and 2 were removed from the data of Sects. 3.1, 3.2 and 3.3 respectively. It means that the data in the third case is more correlated than in the two other cases and that the data in the case 2 has the less correlation. Three different covariance functions were used according to Eq. (4), corresponding to the spectral content of the data in each of the three sections.

Table 1 Distribution and number of simulated T_{rr} data

Data set	Data distribution	Number
A1	Complete 2° equal-area grid	10,448
B1	Incomplete 2° equal-area grid (data with $\varphi > 84°$ and $\varphi < -84°$ neglected)	10,398
C1	Incomplete 2° × 2° equi-angular grid (data with $\varphi > 84°$ and $\varphi < -84°$ neglected)	15,300
D1	On realistic GOCE orbit, selected closest (up to 30 km) to the nodes of the 2° equal-area grid	8,500
E1	On realistic GOCE orbit, selected closest (up to 50 km) to the nodes of the 2° equal-area grid	9,686

The numerical results are given in terms of (a) the error estimate $\sigma(C_{ij})$

$$\sigma(C_{ij}) = \sqrt{\mathrm{ecov}(ij, ij)} \tag{10}$$

of the computed spherical harmonic coefficients, and (b) of the error-correlations according to (9). For the computation of the error-correlations the error estimates of the coefficients are taken directly into account. In (10) i is equal to 25–90 for Sect. 3.1, 51–90 for Sect. 3.2, 3–90 for Sect. 3.3, and j is equal to −90 to 90 for all Sect. 3.

Since the number of the error-correlations is extremely large even between the degrees 51 and 90, these results are given in terms of minimum and maximum values for all degrees and orders and in plots of the error-correlations of the coefficients C_{ij} with all other computed coefficients.

3.1 Experiments using data with uncorrelated noise

For the numerical experiments of this section T_{rr} data were used as observations, i.e., the covariance functions were evaluated for this kind of data. Noise standard deviation equal to 0.01E was assumed for all these data sets. The distribution and the number of data points used in the corresponding numerical experiments are shown in Table 1.

The reason for choosing the upper limit of 90 is that above this degree the error estimates becomes equal to or larger than the signal standard deviations, due to the limited number of data points used in the experiments. Error-covariances of the estimates of spherical harmonic coefficients were computed from degree 25 till 90. The number of the computed error-covariances for each data distribution of Table 1 was equal to 29,310,996.

In Fig. 1, the error-estimates computed with the data distributions of Table 1 are shown. It is seen that for all data distributions the error estimate of the zonal harmonics is increasing with increasing degree. The error estimates of zonal harmonics shown in Fig. 1(B1) is higher comparing to that of (A1), obviously due to the lack of data in the polar caps. In Fig. 1(B1) and (C1), it is shown that with the same lack of the data in the polar caps the error estimates of the zonal harmonics are about the same, in spite of the larger (about 47%) amount of data points of the equiangular relative to the equal-area distribution. This result supports the conclusions by Sneeuw and van Gelderen in Sneeuw and van Gelderen (1997). However, the extra data (compared to the equal-area case) appear to add something to the estimation, reducing the error estimates of sectorial coefficients of orders from ∼35 to ∼70 as Fig. 1 indicates, and are not completely useless.

The error-estimates become very large for the lower harmonics and especially for the zonal harmonics in the case of the experiment (D1) (see Fig. 1), where T_{rr} data on realistic

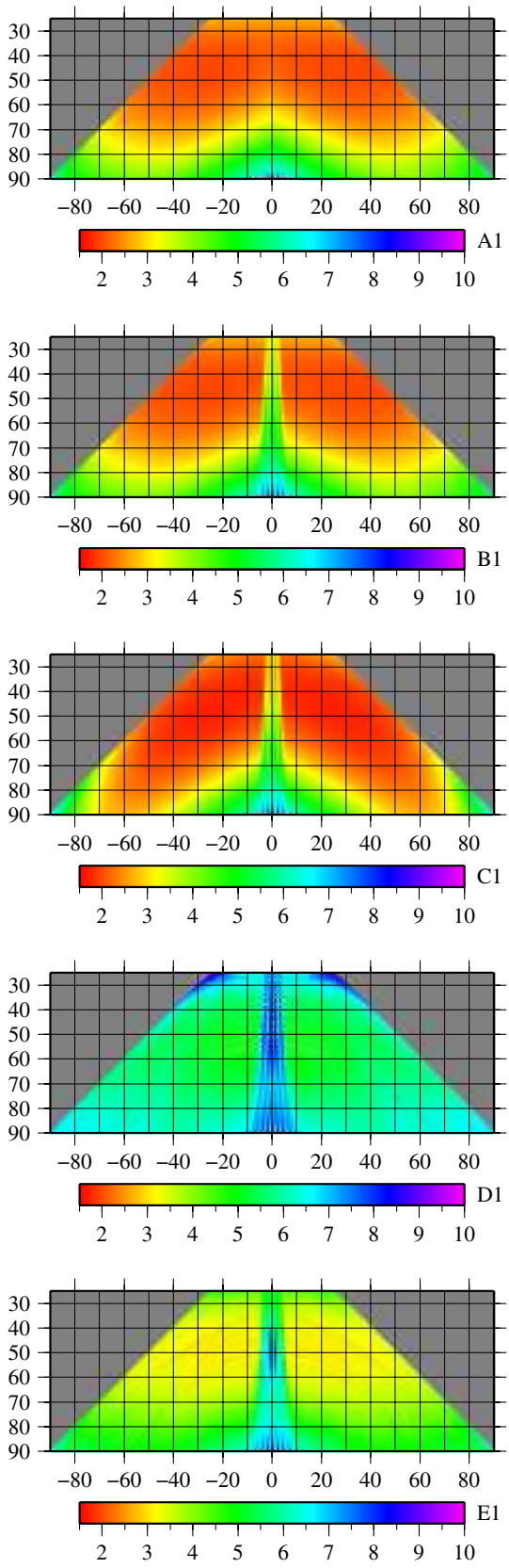

Fig. 1 Error estimates $\sigma(C_{ij})$ (dimensionless), computed from the data distributions of Table 1. All values are multiplied by 10^9

Table 2 Maximum negative and positive error-correlations of the estimates of $\sigma(C_{ij})$, (i = 25–90, j = −90 to 90) with $\sigma(C_{kl})$, (k = 25–90, l = −90 to 90 of the corresponding harmonic coefficients computed with the data distributions of Table 1

Data set	C_{ij}	C_{kl}	Maximum negative correlation	C_{ij}	C_{kl}	Maximum positive correlation
A1	$C_{89\,01}$	$C_{87\,01}$	−0.40	$C_{90\,00}$	$C_{88\,00}$	0.58
B1	$C_{90\,-08}$	$C_{88\,-08}$	−0.33	$C_{47\,00}$	$C_{45\,00}$	0.82
C1	$C_{90\,-37}$	$C_{88\,-37}$	−0.43	$C_{47\,00}$	$C_{43\,00}$	0.80
D1	$C_{41\,-07}$	$C_{39\,-07}$	−0.70	$C_{59\,-01}$	$C_{53\,-01}$	0.78
E1	$C_{41\,-07}$	$C_{39\,-07}$	−0.41	$C_{47\,-01}$	$C_{43\,-01}$	0.88

GOCE orbit were selected close to the nodes of an equal-area grid. This situation was improved in the case of experiment (E1) (see Fig. 1), when, allowing a larger collection radius, more data points were collected.

In Table 2, for the coefficients computed with the data distributions of Table 1, the maximum negative and positive values of error-correlations of the estimates $\sigma(C_(ij)$, (i = 25–90, j = −90 to 90) with $\sigma(C_{kl})$, (k = 25–90, l = −90 to 90) of the corresponding coefficients are shown. Error-correlations between coefficients of the same degree and order, which in the following will be referred as error auto-correlations, are not included in this table. Furthermore, in Table 2 it is shown that minimum and maximum values of error-correlations appeared between coefficients of the same order. Note the very low orders related to maximum positive error-correlations.

For the distribution on an equal-area grid, the maximum negative and positive correlations are changing passing from a complete (A1) to an incomplete (B1) grid with data missing in the polar caps. The maximum positive correlation was increased by about 41%. For the incomplete equal-area (B1) or equiangular (C1) grids the maximum positive error-correlations are very close, occurring between coefficients of neighboring degrees and orders, but it is not valid for the maximum negative correlations.

Finally, in the case of the distribution on a realistic GOCE orbit (D1 and E1 in Table 1), the error-correlations seem to be dependent on the density of the data used. Increasing the number of the data from D1 to E1 by 14%, the maximum negative error-correlation was changed from −0.70 to −0.41 (about 41%), and the maximum positive one was changed by about 12% as it is shown in Table 2.

Since uncorrelated noise was adopted for the input data, dependencies of the error-correlations from the character of the data noise could not be determined.

In Figs. 2, 3, 4, 5, and 6, the error-correlations ecorr(ij, rt) for the experiments carried out with the data of Table 1 are shown. The degree i and the order j of the first coefficient are chosen as in Table 2, the degree r of the second coefficient can vary from 25 to i, while the order t is kept fixed at the value of j. In this way the minimum and the maximum error-correlations of Table 2 are included in the figures.

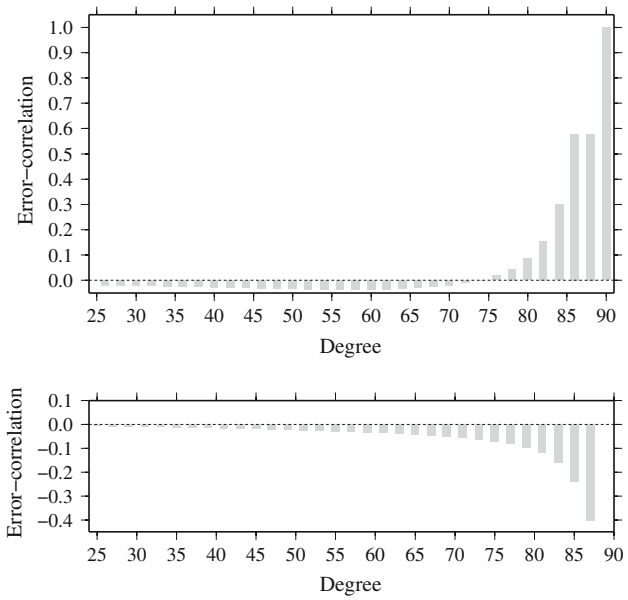

Fig. 2 Solution A1. *Top* Error-correlations of degree 90 and order 0 with all coefficients between degree 25 and 90 and order 0. *Bottom* Error-correlations of degree 89 and order 1 with all coefficients between degree 25 and 89 and order 1

Significant values of error-correlations in the case of the distribution on the complete equal area grid (A1) are restricted to the higher zonal harmonics (degrees > 80) as it is shown in Fig. 2. This is not valid for the incomplete grids (B1) and (C1). The error-correlations in this case are progressively increasing up to the maximum, starting from the lower degree (see Figs. 3, 4). As it was expected the maximum error correlation in the complete equal-area grid is lower comparing to all other distributions of Table 1.

In Figs. 3 and 4 it is shown that for the distribution on an incomplete equal-area (B1) or equiangular (C1) distribution, maximum error-correlations of the zonal harmonics, varying between 0.6 and 0.8 lie between the starting and the middle degrees of the harmonic expansion with a trend towards an increasing error correlation with increasing degree.

Almost similar behavior is valid for the distributions on realistic GOCE orbit (D1 and E1) as it is shown in Figs. 5 and 6. In the case of (D1) the variations of the maximum

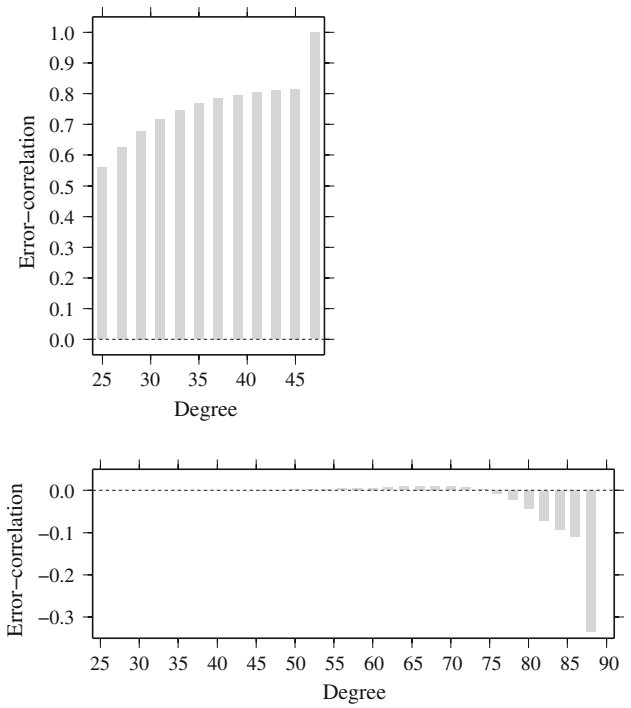

Fig. 3 Solution B1. *Top* Error-correlations of degree 47 and order 0 with all coefficients between degree 25 and 47 and order 0. *Bottom* Error-correlations of degree 90 and order −8 with all coefficients between degree 25 and 90 and order −8

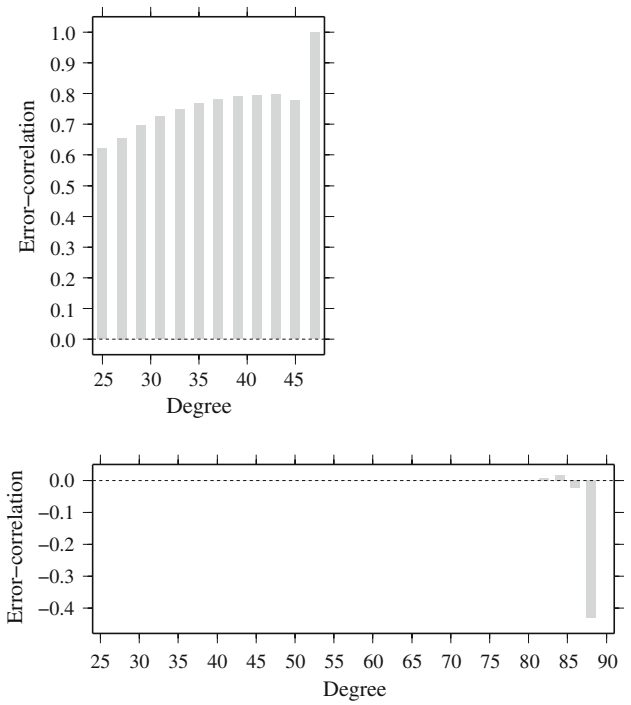

Fig. 4 Solution C1. *Top* Error-correlations of degree 47 and order 0 with all coefficients between degree 25 and 47 and order 0. *Bottom* Error-correlations of degree 90 and order −37 with all coefficients between degree 37 and 90 and order −37

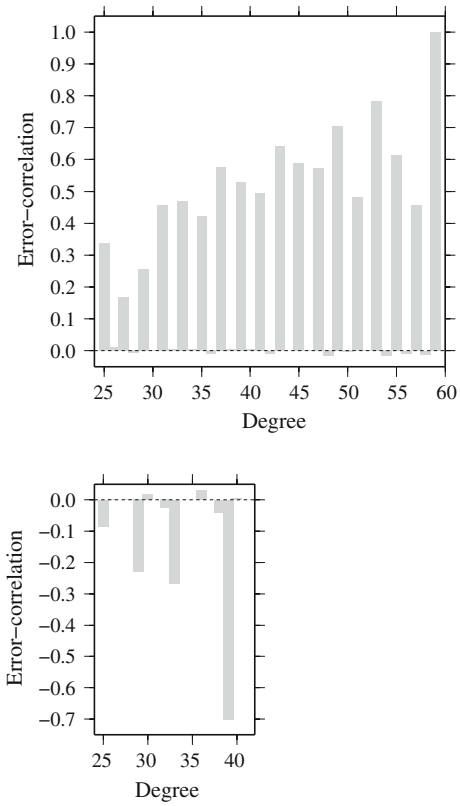

Fig. 5 Solution D1. *Top* Error-correlations of degree 59 and order −1 with all coefficients between degree 25 and 59 and order −1. *Bottom* Error-correlations of degree 41 and order −7 with all coefficients between degree 25 and 41 and order −7

error-correlation are ranging between 0.15 and 0.78, while these are more uniform in the case of (E1), ranging between 0.45 and 0.88.

In all other cases most of the error-correlations are very small to negligible. This is due to the almost grid-like distribution of the data and the approximately symmetric data distribution with respect to the Equator. For instance, the minimum and maximum error-correlations of C_{9090} with all coefficients C_{ij} with $i = 25$–90, $j = -90$ to -90 for the solution (E1) are -0.12 and 0.08 respectively (see Fig. 7) and all other are negligible. For the same solution from the amount of 1927 error-correlations of C_{5001} with all coefficients C_{ij} with $i = 25$–50, $j = -50$ to -50, 51.3% lie between -0.05 and 0, 47.9% between 0 and 0.05 and the rest 0.8% (16 values) between 0.4 and 0.8 (see Fig. 8).

3.2 Experiments using data with correlated noise

In the following numerical experiments, the data points were selected only on realistic GOCE orbit data set covering a time period of 2 months, with correlated noise, using different selection criteria as it is described in Arabelos and Tscherning (2007). The noise added by ESA, based on the

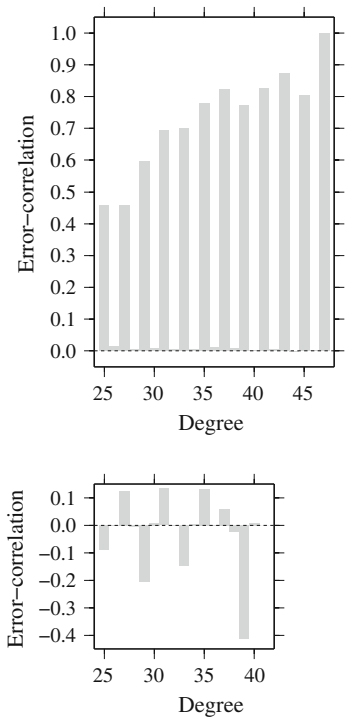

Fig. 6 Solution E1. *Top* Error-correlations of degree 47 and order −1 with all coefficients between degree 25 and 47 and order −1. *Bottom* Error-correlations of degree 41 and order −7 with all coefficients between degree 25 and 41 and order −7

a-priori Fourier spectrum characteristics of GOCE was partially removed as shown by the "POLIMI" GOCE-HPF group (Reguzzoni and Tselfes 2006) after a Wiener filtering. In the experiments the remaining correlated noise was represented by a finite error covariance function (Sansò and Schuh 1987) with noise variance equal to $(0.01337\text{E})^2 = 0.0001787\text{E}^2$ and an along track correlation distance equal to 7°. Note that for gridded data the correlation was spatial (i.e., distance dependent) and not "along track".

Error-covariances of the estimates of spherical harmonic coefficients were computed from degree 51 to 90. The number of the computed error-covariances for each distribution of Table 3 was equal to 16,134,040. In Fig. 9, the error estimates $\sigma(C_{ij})$ for the experiments carried out with the data of Table 3 are shown.

A comparison of Fig. 9 with the Fig. 1 shows that generally, the error-estimates $\sigma(C_{ij})$ in the experiments of Sect. 3.2 are considerably smaller than the $\sigma(C_{ij})$ of Sect. 3.1. This comment will be further discussed after the presentation of the resulting error-correlations.

In Table 4, for the coefficients computed with the data distributions of Table 3, the maximum negative and positive values of error-correlations of the estimates $\sigma(C_{ij})$, (i = 51–90, j = −90 to 90) with $\sigma(C_{kl})$, (k = 51–90, l = −90 to 90) of the corresponding coefficients are shown.

The same remark as for the Table 2 is valid for Table 4: Minimum and maximum values of error-correlations are shown between coefficients of the same (low) order (again excluding auto-correlations).

On the other hand, the error-correlations in Table 4 are generally smaller than those of Table 2. For instance, minimum and maximum error-correlations for (A2) of Table 4 are considerably smaller (by about 50%) comparing to corresponding for (E1) of Table 2, although the same distribution and number of data was used in this case in both experiments.

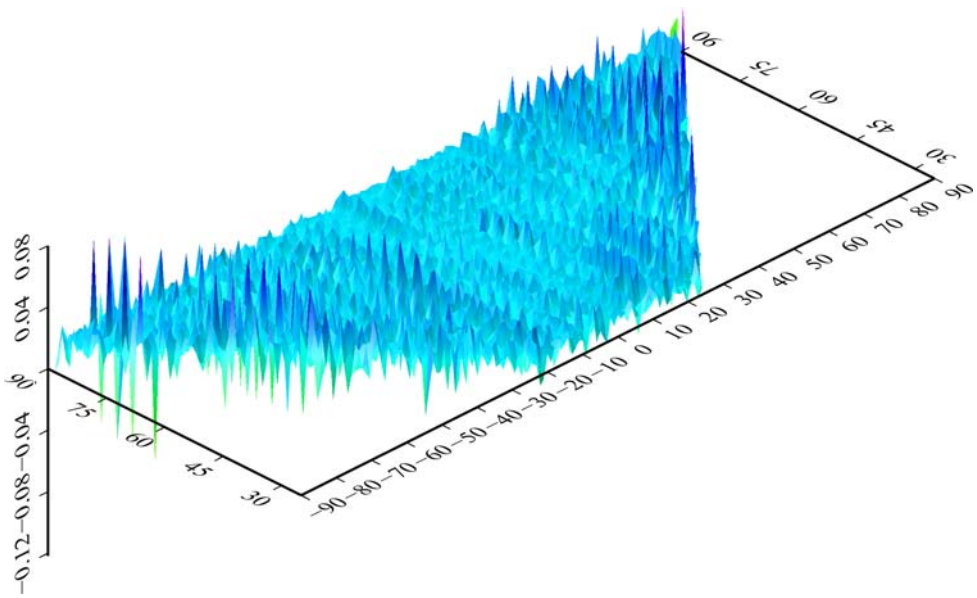

Fig. 7 Solution E1. Error-correlations of C_{9090} with all coefficients C_{ij} and with i = 25–90, j = −90 to 90. Minimum and maximum error-correlations are equal to −0.12 and 0.08 respectively. Many of the error-correlations are very close to zero

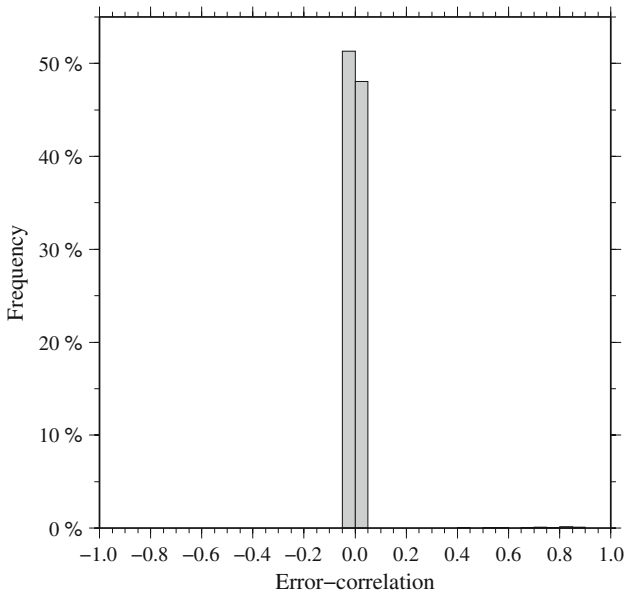

Fig. 8 Solution E1. Distribution of error-correlations of C_{5001} with all coefficients C_{ij} with $i = 25$–50, $j = -50$ to 50

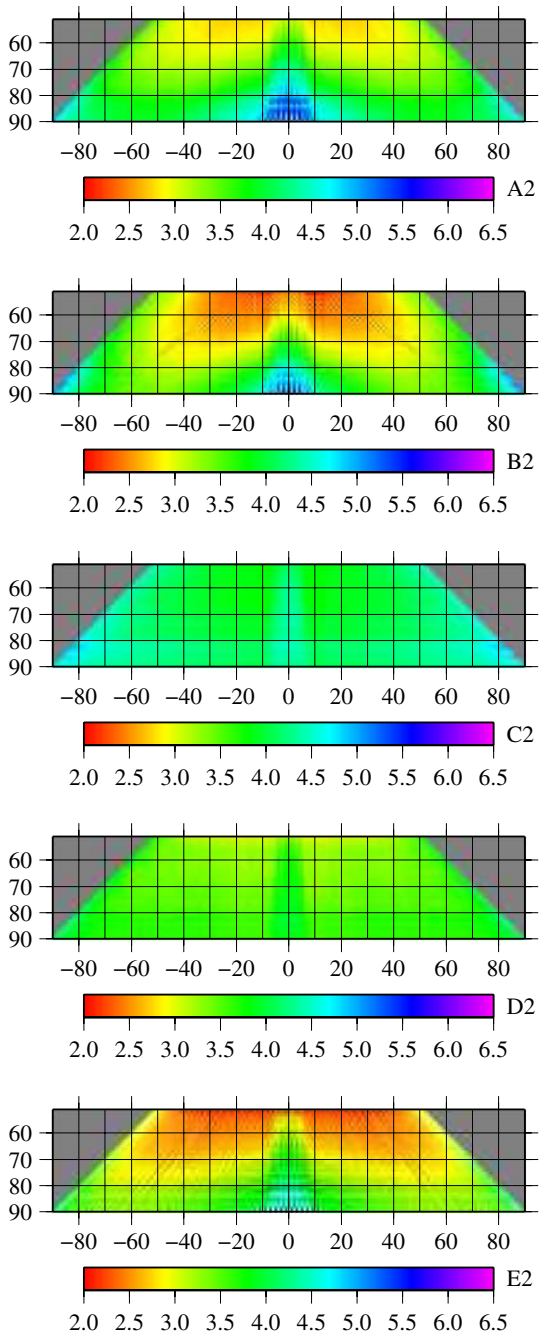

Fig. 9 Error estimates $\sigma(C_{ij})$ (dimensionless), computed from the data distributions of Table 3. All values are multiplied by 10^9

This led to the hypothesis that the error-correlations depend not only on the distribution of the data but also on the covariance function.

The differences between the experiments (E1) and (A2) were (a) the noise (uncorrelated in E1, correlated in A2), (b) the different spectral content of the data (25–360 in E1, 51–150 in A2) and consequently the different signal covariance function used for the prediction of the harmonic coefficients.

On the other hand, the considerable changes in the minimum and maximum values of the error-correlations of the experiments (E1) and (A2) (common parameter is only the data distribution on GOCE realistic orbit) shows that if the data are not distributed on a grid, the variance of the data or the character of the noise have a strong influence on the error-correlations.

In Figs. 10, 11, 12, 13, and 14, the error-correlations ecorr(ij, rt) for the experiments carried out with the data of Table 3 are shown. In these figures the minimum and maximum error-correlations of Table 4 are included.

In all other cases most of the error-correlations between coefficients with different order are very small to negligible. For instance, the minimum and maximum error-correlations for the solution (A2) are -0.08 and 0.06 respectively (see Fig. 15) and all other are negligible.

3.3 Experiments using uncorrelated or correlated noise with the same covariance function

Since with the results of Sects. 3.1 and 3.2 it was not possible to identify the role of each of the varying parameters separately, i.e., of data distribution, covariance function and noise characteristics, a new set of numerical experiments was carried out. In this case, using the same covariance function for all data sets presented in Tables 1 and 3 and uncorrelated or correlated noise, estimates $\sigma(C_{ij})$ and their error-correlations were calculated from degree 3 to 90. The same uncorrelated (like in Sect. 3.1) or correlated (like in Sect. 3.2) noise was adopted also here. The results in terms of maximum

Table 3 Distribution and number of the data

Data set	Data distribution	Number
A2	Selected closest (up to 50 km) to the nodes of the 2° equal-area grid	9,686
B2	Selected closest (up to 50 km) to the nodes of the 2° × 2° equiangular grid	14,131
C2	One point per 2° equal-area block with the largest absolute value of T_{rr}	10,218
D2	Like in C2 but in blocks with var$(T_{rr}) > 0.01\text{E}^2$ the 4 data points closest to the middle of the four 1° sub-blocks were selected	15,340
E2	Selected closest (up to 50 km) to the nodes of the 2° equal-area grid for blocks with var$(T_{rr}) \leq 0.01\text{E}^2$, plus data selected closest to the middle of the four 1° sub-blocks in which each 2° block with var$(T_{rr}) > 0.01\text{E}^2$ was divided	16,601

Table 4 Maximum negative and positive error-correlations of the estimates of $\sigma(C_{ij})$, (i = 51–90, $j = -90$ to 90) with $\sigma(C_{kl})$, (k = 51–90, $l = -90$ to 90) of the corresponding harmonic coefficients computed with the data distributions of Table 3

Data set	C_{ij}	C_{kl}	Minimum correlation	C_{ij}	C_{kl}	Maximum correlation
A2	$C_{89\,-01}$	$C_{87\,-01}$	−0.17	$C_{90\,00}$	$C_{88\,00}$	0.44
B2	$C_{53\,09}$	$C_{51\,09}$	−0.43	$C_{90\,00}$	$C_{86\,00}$	0.47
C2	$C_{79\,32}$	$C_{78\,32}$	−0.08	$C_{66\,02}$	$C_{64\,02}$	0.36
D2	$C_{56\,-38}$	$C_{55\,-38}$	−0.19	$C_{63\,-01}$	$C_{61\,-01}$	0.46
E2	$C_{86\,-58}$	$C_{85\,-58}$	−0.18	$C_{90\,00}$	$C_{88\,00}$	0.50

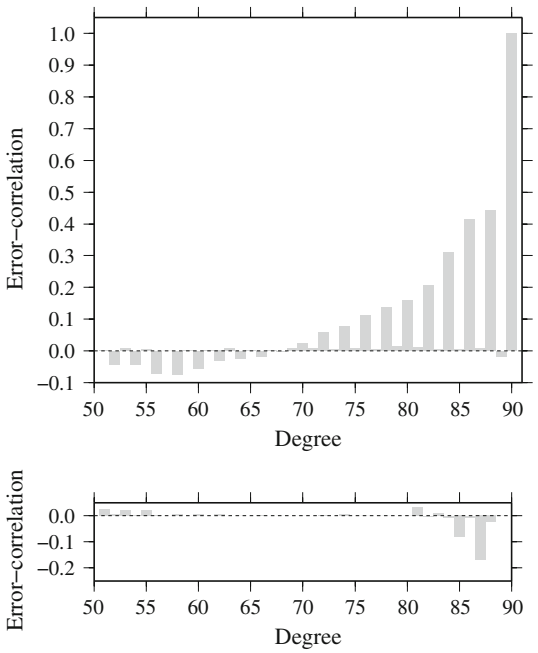

Fig. 10 Solution A2. *Top* Error-correlations of degree 90 and order 0 with all coefficients between degree 51 and 90 and order 0. *Bottom* Error-correlations of degree 89 and order −1 with all coefficients between degree 51 and 89 and order −1

negative and positive values of the error-correlations of the estimates $\sigma(C_{ij})$, ($i = 3$ to -90, $j = -90$ to 90) with $\sigma(C_{kl})$, ($k = 3$ to -90, $l = -90$ to 90) are given in Table 5.

In Table 5, it is shown that for gridded data the error-correlations are larger in the case of correlated than those of uncorrelated noise. The effect of the correlated noise is very strong in the case of the complete equal-area grid (59% for A1) and weaker in the case of the incomplete equal-area or equiangular grid (10% for B1 and 7% for C1). In the case of the data distributed on a realistic GOCE orbit (D1, E1/A2, B2, C2, D2, E2) the effect of the correlated noise is rather weak. But even in this last case, the maximum positive correlations are larger when the noise is correlated.

For gridded data the lack of data in the polar caps plays a pronounced role relating to the magnitude of the error-correlations. This is evident comparing the maximum error-correlations of the experiments (A1), (B1) and (C1) in both Sects. 3.1 and 3.3. In Table 4, the correlation was increased by about 40% from the complete (A1) to incomplete grids (B1) or (C1) while in Table 5 (first part) the corresponding increase was much larger (about 100%). However, the increase is different due to the different covariance functions used in Sects. 3.1 and 3.3.

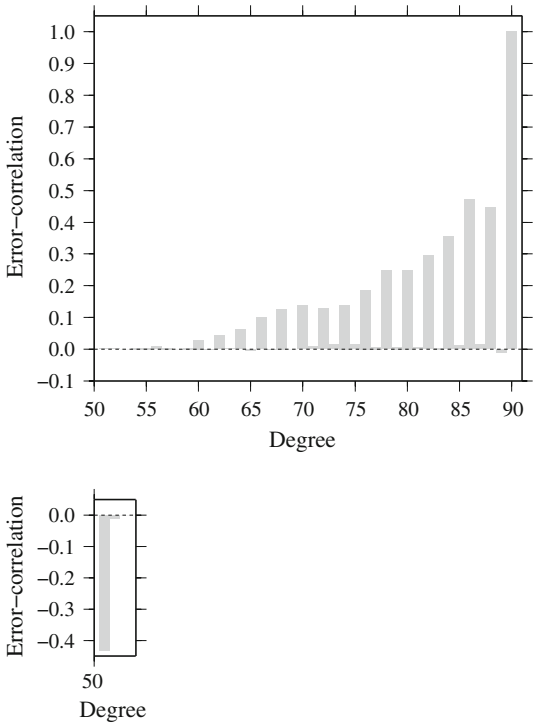

Fig. 11 Solution B2. *Top* Error-correlations of degree 90 and order 0 with all coefficients between degree 51 and 90 and order 0. *Bottom* Error-correlations of degree 53 and order 9 with all coefficients between degree 51 and 53 and order 9

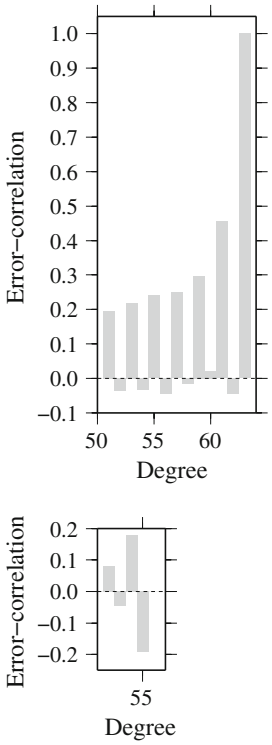

Fig. 13 Solution D2. *Top* Error-correlations of degree 63 and order −1 with all coefficients between degree 51 and 63 and order −1. *Bottom* Error-correlations of degree 56 and order −38 with all coefficients between degree 51 and 56 and order −38

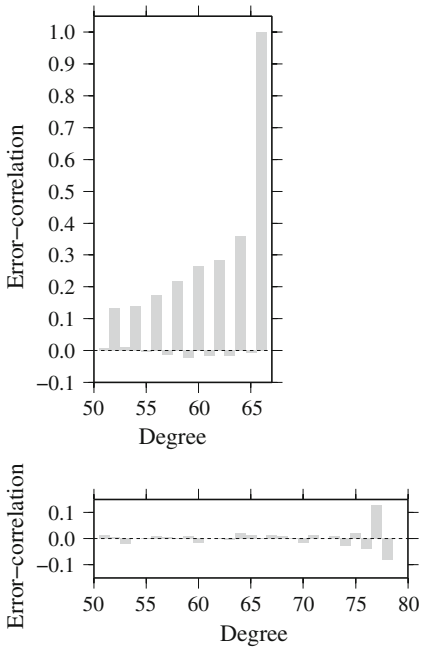

Fig. 12 Solution C2. *Top* Error-correlations of degree 66 and order 2 with all coefficients between degree 51 and 66 and order 2. *Bottom* Error-correlations of degree 79 and order 32 with all coefficients between degree 51 and 79 and order 32

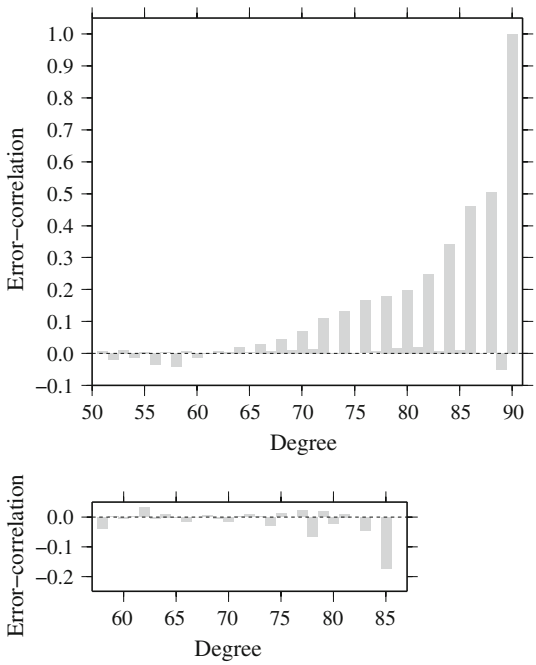

Fig. 14 Solution E2. *Top* Error-correlations of degree 90 and order 0 with all coefficients between degree 51 and 90 and order 0. *Bottom* Error-correlations of degree 86 and order −58 with all coefficients between degree 58 and 86 and order −58

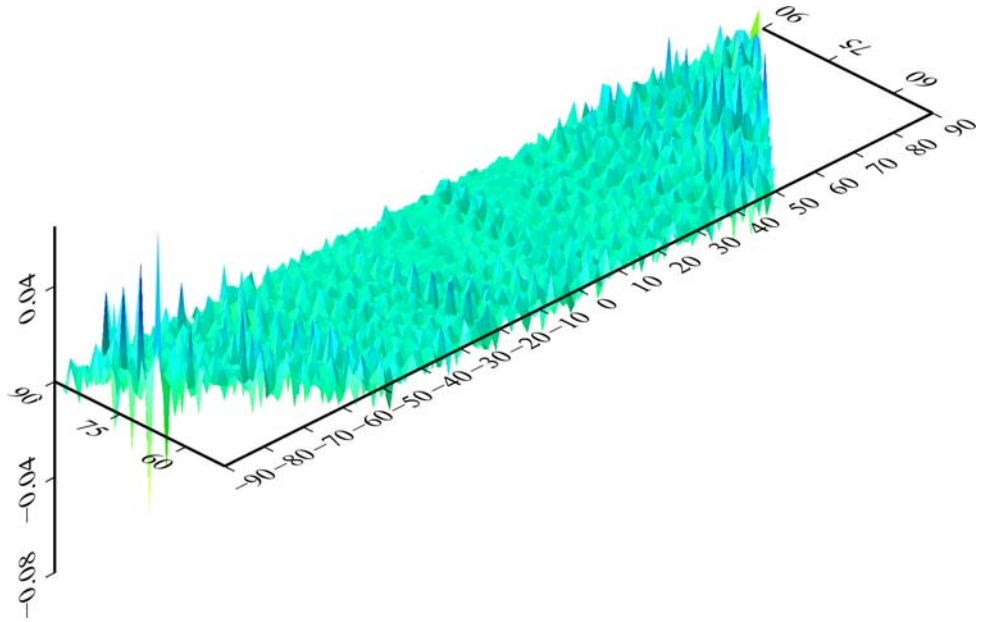

Fig. 15 Solution A2. Error-correlations of C_{9090} with all coefficients C_{ij} with $i = 51$–90, $j = -90$ to 90. Minimum and maximum error-correlations are equal to −0.08 and 0.06 respectively. Most of the error-correlations are equal to or very close to zero

Table 5 Maximum negative and positive error-correlations of the estimates of $\sigma(C_{ij})$, ($i = 25$–90, $j = -90$ to 90) with $\sigma(C_{kl})$, ($k = 25$–90, $l = -90$ to 90) of the corresponding harmonic coefficients, computed with the data distributions of Tables 1 and 3, the same covariance function and with uncorrelated and correlated noise

Data set	C_{ij}	C_{kl}	Maximum negative correlation	C_{ij}	C_{kl}	Maximum positive correlation
Results with uncorrelated noise						
A1	$C_{89\,01}$	$C_{87\,01}$	−0.35	$C_{90\,00}$	$C_{86\,00}$	0.44
B1	$C_{89\,01}$	$C_{87\,01}$	−0.26	$C_{35\,-01}$	$C_{31\,-01}$	0.87
C1	$C_{84\,-31}$	$C_{82\,-31}$	−0.37	$C_{35\,-01}$	$C_{31\,-01}$	0.90
D1	$C_{36\,07}$	$C_{34\,07}$	−0.61	$C_{28\,-01}$	$C_{24\,-01}$	0.82
E1	$C_{38\,-13}$	$C_{36\,-13}$	−0.37	$C_{28\,-01}$	$C_{24\,-01}$	0.89
A2[a]						
B2	$C_{36\,-07}$	$C_{34\,-07}$	−0.61	$C_{28\,01}$	$C_{24\,01}$	0.89
C2	$C_{55\,00}$	$C_{07\,00}$	−0.15	$C_{15\,00}$	$C_{13\,00}$	0.74
D2	$C_{67\,-46}$	$C_{66\,-46}$	−0.16	$C_{17\,00}$	$C_{15\,00}$	0.76
E2	$C_{43\,22}$	$C_{41\,22}$	−0.30	$C_{27\,01}$	$C_{23\,01}$	0.88
Results with correlated noise						
A1	$C_{43\,-01}$	$C_{37\,-01}$	−0.54	$C_{90\,02}$	$C_{86\,20}$	0.70
B1	$C_{42\,-16}$	$C_{40\,-16}$	−0.47	$C_{45\,01}$	$C_{41\,01}$	0.96
C1	$C_{89\,54}$	$C_{87\,54}$	−0.60	$C_{43\,01}$	$C_{37\,01}$	0.96
D1	$C_{36\,07}$	$C_{34\,07}$	−0.62	$C_{28\,-01}$	$C_{24\,-01}$	0.83
E1	$C_{36\,-07}$	$C_{34\,-07}$	−0.34	$C_{28\,-01}$	$C_{24\,-01}$	0.89
A2[a]						
B2	$C_{41\,07}$	$C_{39\,07}$	−0.64	$C_{28\,-01}$	$C_{24\,-01}$	0.89
C2	$C_{55\,00}$	$C_{07\,00}$	−0.17	$C_{17\,00}$	$C_{15\,00}$	0.75
D2	$C_{82\,-55}$	$C_{81\,-55}$	−0.19	$C_{19\,00}$	$C_{17\,00}$	0.79
E2	$C_{74\,40}$	$C_{62\,40}$	−0.26	$C_{35\,-01}$	$C_{33\,-01}$	0.90

[a] The results of A2 are identical to E1, due to same distribution and covariance function

A direct comparison between the results of Table 4 with those of second part of Table 5 (with correlated noise) is not possible, since the maximum negative and positive error-correlations in the last occurred in degrees which are not computed in Table 4.

4 Conclusion

The coefficient error estimates have progressively increasing values for increasing degree and low orders (<10). The highest error-variances are in the zonal harmonics for all distributions examined in the experiments. Furthermore, large values of error estimates appeared for simultaneously maximum degrees and orders. If the data are distributed on equal-area or equiangular grids, many error estimates are very small.

The error-correlations resulting from the error-covariances and the error estimates of the harmonic coefficients show characteristic patterns, depending on the data distribution, the data variance and the character of the noise (correlated or not). For equi-angular gridded data for each degree i and order j, there will be at most $i - j$ non-zero error-covariances, i.e., those of the same order have a non-zero error correlation. Due to the (sometimes approximate) symmetry around the Equator also even–odd and odd–even combinations of the orders leads to zero or close to zero error-covariances.

For non-gridded data maximum values of error-correlations (excluding autocorrelations) are also seen between harmonic coefficients of different degree and same order. This is valid for any distribution used in this study. For a distribution on a complete equal-area grid, error-correlations show their maximum values for degrees close to maximum and orders close to zero. For distributions on incomplete equal-area or equiangular grids, where data in the polar caps are missing, changes in the previous described behavior occurred.

For data distributions on realistic GOCE orbit, but close (up to distances 30–50 km) to the nodes of an equal-area grid, the maximum error-correlations occurred between coefficients of lower degrees (between 40 and 60) and low orders (<10).

For non gridded data, as for instance the distribution on a GOCE realistic orbit, parameters such as the character of the data noise (correlated or not) and the data variance have a significant role in the resulting error-correlations. This shows that the use of equiangular gridded data with uniform uncorrelated noise on each parallel will result in error correlations which may be underestimated compared to more realistic data and noise characteristics with up to 30%, see Table 2. This is useful information for methods using gridded data such for instance FSC.

From this point of view, it is very important to emphasize that using a more localized covariance function, e.g., by subtracting low degree harmonics we may come close to a situation where one obtains very low error-covariances of the estimates of spherical harmonic coefficients even for data distribution on realistic GOCE orbit, including correlated noise.

Acknowledgments We are very thankful for the important comments by the reviewers, helping us to improve the paper.

References

Arabelos DN, Tscherning CC (2007) On a strategy for the use of GOCE gradiometer data for the development of a geopotential model by LSC, Proc. The 3rd International GOCE User Workshop, ESA-ESRIN, Frascati, Italy, 6–8 November 2006 (ESA SP-627, January 2007), pp 69–75

Colombo OL (1981) Numerical methods for harmonic analysis on the sphere, OSU Rep. 310, Columbus

Heiskanen WA, Moritz H (1967) Physical geodesy. W.H. Freeman & Co, San Francisco

Johannesen JA, Balmino G, Le Provost C, Rummel R, Sabadini R, Sünkel H, Tscherning CC, Visser PNAM, Woodworth P, Huges CH, Le Grand P, Sneeuw N, Perosanz F, Aguirre-Martinez M, Rebhan H, Drinkwater M (2003) The European gravity Field and steady-state ocean circulation explorer mission: impact on geophysics. Surv Geophys 24(4):339–386

Lemoine FG, Kenyon SC, Factor JK, Trimmer RG, Pavlis NK, Chinn DS, Cox CM, Klosko SM, Luthcke SB, Torrence MH, Wan YM, Williamson RG, Pavlis EC, Rapp RH, Olson TR (1998) The Development of the Joint NASA GSFC and the National Imagery and Mapping Agency (NIMA) Geopotential Model EGM96, NASA/TP-1998-206861, Goddard Space Flight Center, Greenbelt

Moritz H (1980) Advanced Physical Geodesy. Wichmann, Karlsruhe

Reguzzoni M, Tselfes N (2006) Filtering of the GOCE mission observations. Presented at the EGU General Assembly, Vienna, April 2–7

Sansò F, Schuh W-D (1987) Finite covariance functions. Bull Géod 61(4):331–347

Sansò F, Tscherning CC (1980) Notes on convergence in collocation—theory. Boll Geod Sci Affini N 3:221–252

Sansò F, Tscherning CC (2003) Fast spherical collocation - theory and examples. J Geod 77:101–112, DOI:10.1007/s00190-002-0310-5

Sneeuw N, van Gelderen M (1997) The polar gap, in geodetic boundary value problems in view of the one Centimeter Geoid. In: Sansò F, Rummel R (eds) Lecture Notes in Earth Sciences, vol 65. Springer, Berlin

Tscherning CC (2001) Computation of spherical harmonic coefficients and their error estimates using Least Squares Collocation. J Geod 75:14–18